Use of Magnetic Nanoparticles as Nanosensors to Probe for Molecular Interactions

J. Manuel Perez, Lee Josephson, and Ralph Weissleder*[a]

Biocompatible magnetic nanosensors have been designed to detect molecular interactions in biological media. Upon target binding, these nanosensors cause changes in the spin – spin relaxation times of neighboring water molecules, which can be detected by magnetic resonance (NMR/MRI) techniques. These magnetic nanosensors have been designed to detect specific mRNA, proteins, enzymatic activity, and pathogens (e.g., virus) with sensitivity in the low femtomole range (0.5 – 30 fmol).

Introduction

The development of nanoparticles of metals and semiconductors has been extensively pursued in recent years because of their unique optical, electronic, and magnetic properties.[1, 2] When coupled to affinity ligands, such nanoparticles can function as sensitive biological nanosensors. For example, gold nanoparticles[3, 4] and CdSe quantum dots[5–7] have been conjugated with synthetic oligonucleotides, proteins, and other ligands to create colorimetric and fluorescent nanosensors. We are interested in alternative detection technologies and have developed magnetic nanosensors composed of magnetic nanoparticles that can be used to detect molecular interactions by magnetic resonance (NMR/MRI) techniques. When these magnetic nanoparticles bind to their intended molecular target, they form stable nanoasemblies; this leads to a corresponding decrease in the spin – spin relaxation time (*T2*) of surrounding water molecules.[8] We have built on this observation and have developed sensitive, homogenous assays to detect a variety of different molecular interactions in biological samples with minimal or no sample preparation. In one study, we showed detection thresholds for DNA and proteins at the low femtomole level (0.5 fmol) in unpurified samples,[9] whereas in other studies we have been able to detect enzymatic activities such as that of restriction endonucleases[10] and proteases.[9, 11]The technology has also been used to sense different types of reversible molecular interactions such as DNA – DNA, DNA – protein, protein – protein, protein – small molecule, and enzymatic reactions. These magnetic nanosensors are particularly suited for screening a specific target in a biological media such as green fluorescent protein (GFP) mRNA in cell lysate,[9] or a specific viral particle (HSV-1) in serum samples.[12] They could also provide a superior method for investigating many problems in proteomics, system biology and, potentially, for in vivo imaging.

Magnetic Nanosensor Composition

These previously developed nanosensors are composed of 3 – 5 nm *m*onocrystalline *i*ron *o*xide *n*anoparticles (MION), with an inverse spinel structure (cubic close packed) of $(Fe_2O_3)_n(Fe_3O_4)_m$, surrounded with a 10 kDa dextran coating approximately 10 nm thick.[13] The average size of the nanoparticles, as determined by light scattering, is about 25 – 30 nm, depending on the preparation. This size is equivalent to a 750 – 1 200 kDa globular protein. Different MION preparations have a blood half-life of >10 h in mice. Related clinical nanoparticle preparations have circulation times of 24 h in humans.[14] In order to develop more stably coated and amino-functionalized sensors, the dextran coating has been cross-linked with epichlorohydrin, and then treated with ammonia to provide functional amino groups.[15] Preparations of the resulting aminated cross-linked iron oxide nanoparticle (amino-CLIO) have about 40 amino groups per particle with an average particle size of 40 – 50 nm. These nanoparticles can withstand harsh treatment, such as incubation at 120 °C for 30 minutes, without a change in size or loss of their dextran coat. Amino groups in amino-CLIO can react by N-hydroxysuccinimide (NHS) based bifunctional cross-linking, allowing attachment of a range of sulfhydryl-bearing biomolecules. This gives rise to biomolecule – nanoparticle conjugates with unique biological properties, as compared to simple polymer coated iron oxide nanoparticles. Apart from their use as sensors, the resultant superparamagnetic nanoparticles have been shown to be valuable for imaging specific molecular targets, [16–18] and as reagents for cell labeling and tracking.[15, 19]

Mechanism of Magnetic Relaxation Switching

The iron oxide crystal core in CLIO is superparamagnetic, becoming magnetized when placed in an external magnetic field.[13] The combined electron spins in the crystal produce a single large magnetic dipole, creating a local magnetic-field

[a] *Dr. J. M. Perez, Dr. L. Josephson, Dr. R. Weissleder*
Center for Molecular Imaging Research, Massachusetts General Hospital
Harvard Medical School, Building 149
13th Street, 5404, Charlestown MA 02129 (USA)
Fax: (+1) 617-726-5708
E-mail: weissleder@helix.mgh.harvard.edu

 DOI: 10.1002/cbic.200300730 © 2004 Wiley-VCH Verlag GmbH & Co. KGaA, Weinheim

gradient and therefore an inhomogeneity in the external magnetic field. Water protons diffusing within the local inhomogeneity precess at an off-resonance frequency, dephasing their spins, thus increasing the relaxation rate (1/*T2*) as described by outer-sphere theory, in which 1/*T2* is directly proportional to nanoparticle cross-sectional area.[20, 21] We hypothesize that, when individual superparamagnetic nanoparticles assemble into clusters and the effective cross sectional area becomes larger, the nanoassembly becomes more efficient at dephasing the spins of surrounding water protons, leading to an enhancement of the relaxation rates (1/*T2*). Hence, the reference to the magnetic nanosenors as magnetic relaxation switches (Figure 1). Interestingly, since the spin-lattice relaxation time (*T1*) is

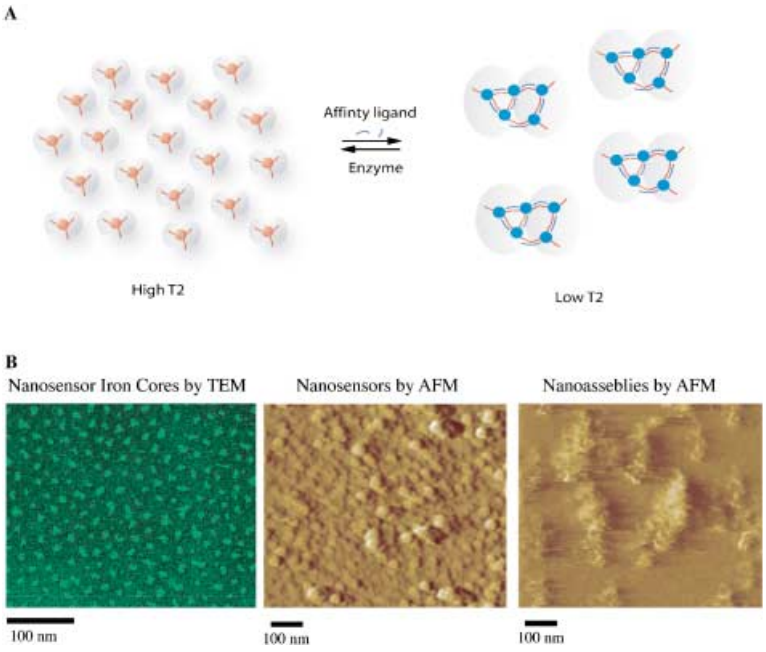

Figure 1. *A. Diagram of the magnetic nanosensors acting as magnetic relaxation switches. Superparamagnetic nanoparticles self-assemble in the presence of a target with a corresponding decrease in the solution* T2 *relaxation time. Self-assembled nanoparticles can be dispersed by the action of an enzyme, temperature or pH change depending on the nature of the bond holding the nanoassembly together. B. Transmition Electron Microscopy (TEM) and Atomic Force Microscopy (AFM) images of a monolayer of nanosensors. TEM shows the iron oxide crystal cores with an average diameter of 8 nm. AFM of a similar monolayer shows the cross-linked dextran shell of nanoparticles, with an average particle size of 50 nm. Upon target recognition, CLIO forms nanoassemblies of 200 – 300 nm.*

independent of nanoparticle assembly formation,[8] this parameter can be used to measure concentration in both nanoassembled and dispersed states within the same solution. Nanoassembly formation can be designed to be reversible (e.g., by temperature, chemical cleavage, pH etc.) so that "forward" or "reverse" assays can be developed. The following sections describe specific examples of forward (clustering) or reverse (declustering) types of assays for detecting a large variety of biologically relevant materials.

Detecting DNA

We have performed a number of experiments to detect oligonucleotide sequences.[8, 9] In these experiments, we coupled an average of three oligonucleotides (12 base pairs) to the nanoparticles using *N*-succinimidyl-3-(2-pyridyldithio)propionate (SPDP) as a linker. For each intended target sequence, we made two unique nanoparticle populations (termed P1 and P2), recognizing adjacent 24 base pair long target sequences. Cluster formation of these nanoparticles, upon addition of a complementary oligonucleotide, resulted in a quick and significant decrease in the spin – spin relaxation times (*T2*) of neighboring water molecules, as measured with a 0.47 T NMR bench-top relaxometer at 40 °C (Figure 2 A). When a noncomplementary oligonucleotide was used, no change in *T2* was observed. The average decrease in *T2* was linear with the amount of DNA added in the concentration range displayed (Figure 2 A, insert). Similar changes in *T2* relaxation times were observed when the experiments were conducted in turbid solution. The observed changes in *T2* were sensitive to temperature cycling. Hybridization was minimal at 80 °C, therefore no or minimal changes were observed in *T2*. The effect of multiple cycles of heating (80 °C) and cooling (40 °C) on *T2* are shown in Figure 2 B. When dithiothreitol (DTT), a reducing agent capable of cleaving the oligonucleotide off the nanoparticle, was added to the solution, *T2* relaxation times returned to baseline values, and no change in *T2* was observed during temperature cycling. To investigate the detection threshold and selectivity of P1 and P2 sensors for a given oligonucleotide sequence, we performed experiments at a higher magnetic field strength (1.5 T). For these experiments a 24 bp oligonucleotide targeting the GFP mRNA was selected. At 1.5 T, significant differences were readily apparent by MRI between the samples in the low femtomole range (0.5 – 2.7 fmol).[9] In addition, we were able to detect single and multiple nucleotide mismatches as well as single and multiple insertions. GFP mRNA, in a mixture of isolated total RNA and cell lysate, was easily detected from a panel of GFP-transfected cell lines (Figure 3 A and 3 B). In addition, changes detected in *T2* for GFP-transfected cells correlated with the GFP fluorescence of the cell lines (Figure 3 C).

Detecting Proteins

To extend the observations described above, we then tested whether magnetic nanosensors can be designed to detect a specific protein in solution by using antibody-mediated interactions. First, we prepared avidin-P1 conjugates as generic reagents for attachment of any biotinylated antibody (or peptide) to the nanosensor. On average, each nanoparticle contained two avidins (i.e., eight binding sites) as described in detail elsewhere.[9] Biotinylated anti-GFP polyclonal antibody was then attached to yield a GFP-sensitive nanosensor. When the nanosensors were used to probe for GFP protein, significant changes in *T2* relaxation time were observed. These changes were time and dose dependent. Incubation with control protein (BSA) showed no significant changes in *T2*. Similar observations were also made by using several alternative model systems:

 © 2004 Wiley-VCH Verlag GmbH & Co. KGaA, Weinheim

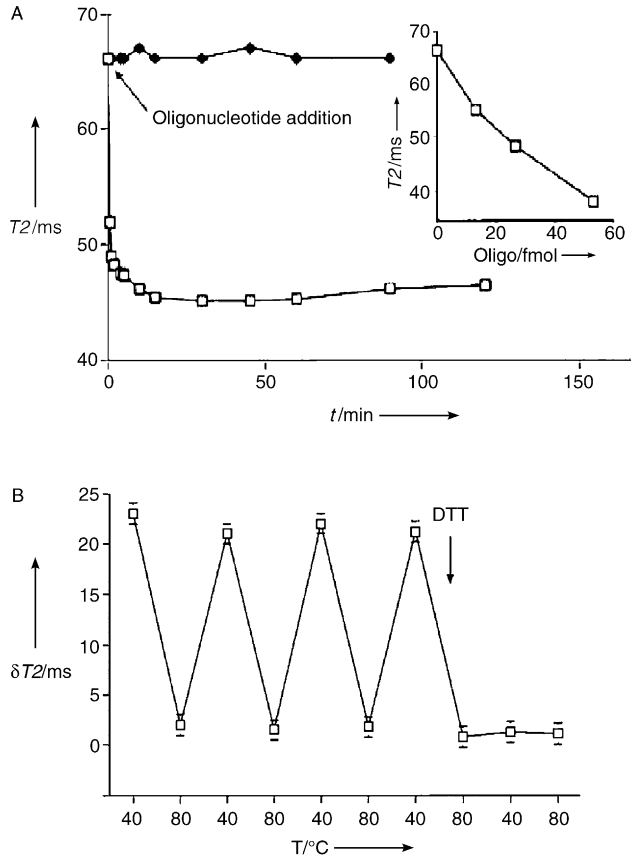

Figure 2. *A. Temporal change of water* T2 *relaxation times with (□) and without (◆) complementary oligonucleotide. Insert shows the effect of increasing concentrations of oligonucleotides on water* T2. *B.* T2 *changes (δ*T2*) of an aqueous solution of nanosensors as a function of temperature cycling. Reprinted with permission from ref. [8].*

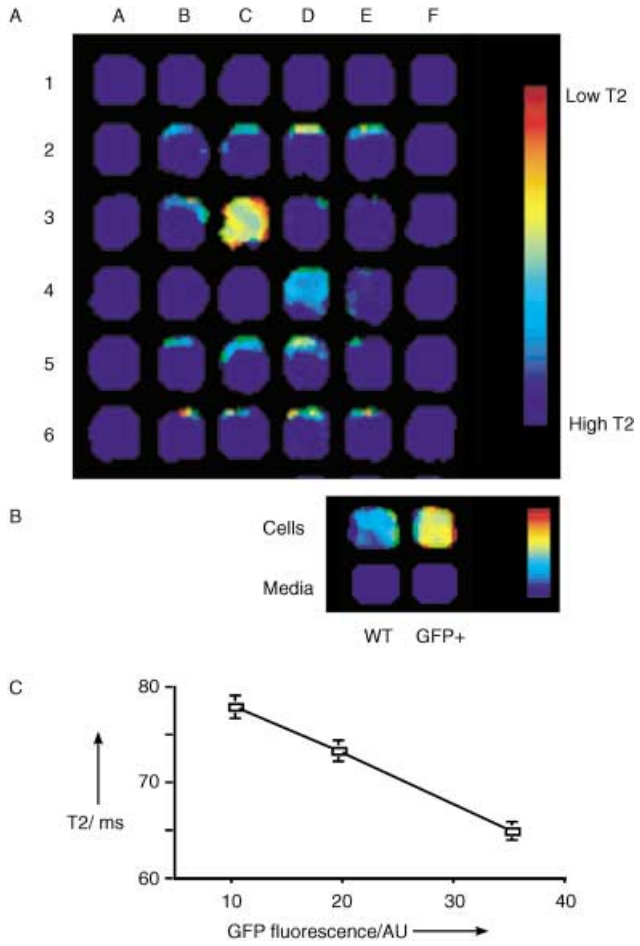

Figure 3. *A. GFP mRNA detection in a panel of GFP trasfected cells using MRI. Total RNA was extracted and mixed with GFP sensitive nanosensors in a 384 well plate and imaged by MRI at 1.5 T. Wells C3 and D4 correspond to GFP+ cell lines known to express different levels of GFP mRNA. B. MR image of GFP mRNA expression in cell lysate. C. GFP fluorescence and* T2 *measurements of GFP mRNA show high correlation in whole cell lysate experiments. Reprinted with permission from ref. [9].*

1) probing CA-125 protein with an anti-CA125 antibody and 2) testing avidin–biotin interactions as model for protein–small-molecular-weight molecule interactions. In all of these experiments, *T2* changes were observed with detection limits of target protein in the low femtomol range (1–10 fmol).

Detecting Enzymatic Activity

We have also developed magnetic nanosensors for measuring various enzymatic activities including restriction endonucleases, methylases, and proteases.[9–11] We hypothesized that a restriction endonuclease such as *Bam*HI (by cleaving the double-stranded oligonucleotide linking P1 and P2) would cause a designed nanoassembly to switch to a dispersed state and produce an increase in *T2*.[10] For these experiments, two sets of magnetic nanoparticles (P1 and P2) were designed so that they would hybridize to each other forming a *Bam*HI recognition site. As expected, a decrease in *T2* was observed when P1 and P2 were mixed together (Figure 4) since oligonucleotides on the two sets of nanoparticles hybridize forming a *Bam*HI-sensitive nanoassembly. Incubation with *Bam*HI resulted in an increase in *T2* back to baseline levels. Other endonucleases such as *EcoR*I,

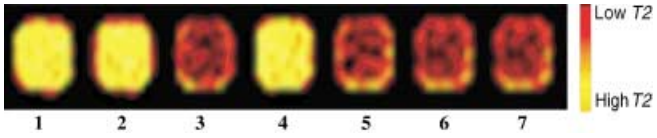

Figure 4. *NMR imaging of enzymatic activity. Restriction endonuclease detection using a pair of nanosensors with complementary oligonucleotides (1 and 2). When mixed in solution the oligonuleotides hybridize causing the nanosensors to cluster (3). A* Bam*HI sensitive nanoassembly, with a corresponding decrease in* T2*, is formed. Upon treatment with* Bam*HI, the nanoassemblies disassemble, and an increase in T2* is observed (4). Treatment with other restriction endonucleases (Eco*RI*, Hind*III*, Dpn*I*) do not cause a change in* T2 *of the solution (5, 6, 7).*

*Hind*III, and *Dpn*I did not cause an increase in *T2* when incubated with the *BamH*I-sensitive nanoassembly. Additional experiments utilizing a combination of *dam* methylase and a series of methylation-sensitive restriction endonucleases show that the double-stranded oligonucleotide sequence holding the nanoassembly together can be methylated as normal. The methylation event can be detected by addition of a methylation-

 © 2004 Wiley-VCH Verlag GmbH & Co. KGaA, Weinheim

sensitive restriction endonuclease.[9] In a similar fashion, we have extended the technology to sense different proteases. In the first assay, a magnetic nanoparticle containing a biotinylated caspase-3-specific peptide substrate (P2), was prepared and incubated with avidin-P1 to form a caspase-3-sensitive magnetic nanoassembly.[9] The peptide substrate is specifically recognized by caspase-3, thus serving as an assay for this enzyme. As shown, the caspase-3-mediated reaction was associated with a dose-dependent increase in the *T2* relaxation time with kinetics similar to those reported with fluorogenic substrates. The two-step assay employs peptide substrates with a protease recognition sequence flanked by one biotin molecule at each terminus.[11] The double-biotinylated peptide substrates interact with Avidin-P1 creating a nanoassembly. When treated with a specific protease, the peptide substrate is cleaved, the two biotins are separated, and the reaction products no longer cluster the Avidin-P1 nanosensors. By using this approach, magnetic nanoassemblies responsive to trypsin, renin, and matrix metalloprotease-2 activity have been developed and tested.[11]

Detecting Viruses

Recently, we reported the construction of magnetic nanosensors capable of detecting a more complex target, such as intact viral particles in serum.[12] Since we have already shown that proteins are readily detected by using this technique, we reasoned that magnetic nanoparticles coated with antibodies against virus surface proteins could be used to detect the viral particle in solution. We hypothesized that the multiple interactions that occur between a multivalent target (virus) and a multivalent magnetic nanoparticle – antibody conjugate could result in a highly sensitive assay for the detection of viruses. Using this approach, we have been able to detect low levels (five viral particles in 10 μL) of herpes simplex virus-1 (HSV-1) and adenovirus-5 (ADV-5) in serum solutions.[12] These model viral particles were selected for our studies because they represent a reasonable surrogate model for other more pathogenic viruses, and are currently used as viral vectors in gene-therapy studies. The magnetic viral-detection method represents an improvement over current PCR methods[22] as it is fast, less prone to artifacts, and does not require removal of proteins or the use of amplifying enzymatic reactions. These viral-specific nanoparticles can potentially be further developed into viral-specific imaging agents that are able to detect the distribution of viruses and perhaps other pathogens in vivo by MRI.

Outlook

The unique detection method of magnetic nanosensor technology developed, allows for rapid detection of a target without extensive purification of the sample or signal amplification. Since light is not used (as in fluorescence, absorbance, chemiluminescence, etc.) it does not affected the outcome of the assay, and experiments can be carried out in turbid, light-impermeable media such as blood, cell suspensions, culture media, lipid emulsions, and even whole tissue. The assay does not require immobilization of the sample onto a flat surface (e.g. microarray glass slides) therefore faster hybridization and binding kinetics are observed. The assay has the flexibility to detect various biomolecular interactions like mRNA, protein, and enzymatic activity simultaneously and can be run in a high-throughput format by using MRI and NMR. At the low iron concentration (<20 μg Fe per mL) used in our experiments, the nanometer-sized clusters do not aggregate and therefore do not precipitate. Finally, since similar iron oxide nanoparticles are currently used in clinical studies and shown to have little to no toxicity,[14] the technology could be applied for in vivo sensing of molecular targets by MRI.

Acknowledgements

We gratefully acknowledge support from the National Cancer Institute by a P50 Center Grant to R.W. (CA86355) and a Career Award to J.M.P. (CA101781).

Keywords: magnetic resonance imaging · molecular recognition · nanosensors · nanostructures · NMR spectroscopy

[1] P. Alivasatos, *Science* **1996**, *271*, 933.
[2] H. Weller, *Angew. Chem.* **1993**, *105*, 43; *Angew. Chem. Int. Ed. Engl.* **1993**, *32*, 41.
[3] C. A. Mirkin, R. L. Letsinger, R. C. Mucic, J. J. Storhoff, *Nature* **1996**, *382*.
[4] R. Elghanian, J. J. Storhoff, R. C. Mucic, R. L. Letsinger, C. A. Mirkin, *Science* **1997**, *277*.
[5] M. Han, X. Gao, J. Z. Su, S. Nie, *Nat. Biotechnol.* **2001**, *19*, 631.
[6] W. C. Chan, S. Nie, *Science* **1998**, *281*, 2016.
[7] X. Wu, H. Liu, J. Liu, K. N. Haley, J. A. Treadway, J. P. Larson, N. Ge, F. Peale, M. P. Bruchez, *Nat. Biotechnol.* **2003**, *21*, 41.
[8] L. Josephson, J. M. Perez, R. W. Weissleder, *Angew. Chem.* **2001**, *113*, 3304; *Angew. Chem. Int. Ed.* **2001**, *40*, 3204.
[9] J. M. Perez, L. Josephson, T. O'Loughlin, D. Hogemann, R. Weissleder, *Nat. Biotechnol.* **2002**, *20*, 816.
[10] J. M. Perez, T. O'Loughin, F. J. Simeone, R. Weissleder, L. Josephson, *J. Am. Chem. Soc.* **2002**, *124*, 2856.
[11] M. Zhao, L. Josephson, Y. Tang, R. Weissleder, *Angew. Chem.* **2003**, *115*, 1413; *Angew. Chem. Int. Ed.* **2003**, *42*, 1375.
[12] J. M. Perez, F. J. Simeone, Y. Saeki, L. Josephson, R. Weissleder, *J. Am. Chem. Soc.* **2003**, *125*, 10192.
[13] T. Shen, R. Weissleder, M. Papisov, A. Bogdanov, Jr., T. J. Brady, *Magn. Reson. Med.* **1993**, *29*, 599.
[14] M. G. Harisinghani, J. Barentsz, P. F. Hahn, W. M. Deserno, S. Tabatabaei, C. H. van de Kaa, J. de la Rosette, R. Weissleder, *N. Engl. J. Med.* **2003**, *348*, 2491.
[15] L. Josephson, C. H. Tung, A. Moore, R. Weissleder, *Bioconjug. Chem.* **1999**, *10*, 186.
[16] D. Hogemann, L. Josephson, R. Weissleder, J. P. Basilion, *Bioconjug. Chem.* **2000**, *11*, 941.
[17] E. A. Schellenberger, A. Bogdanov, Jr., D. Hogemann, R. Weissleder, L. Josephson, J. Tait, *Mol. Imaging* **2002**, *1*, 1.
[18] H. W. Kang, L. Josephson, A. Petrovsky, R. Weissleder, A. Bogdanov, Jr., *Bioconjug. Chem.* **2002**, *13*, 122.
[19] M. Lewin, N. Carlesso, C. H. Tung, X. W. Tang, D. Cory, D. T. Scadden, R. Weissleder, *Nat. Biotechnol.* **2000**, *18*, 410.
[20] R. A. Brooks, *Magn. Reson. Med.* **2002**, *47*, 388.
[21] P. Gillis, F. Moiny, R. A. Brooks, *Magn. Reson. Med.* **2002**, *47*, 257.
[22] S. Nicoll, A. Brass, H. A. Cubie, *J. Virol. Methods* **2001**, *96*, 25.

Received: July 31, 2003 [C730]

 © 2004 Wiley-VCH Verlag GmbH & Co. KGaA, Weinheim